EFFECTIVE IMPEDANCE OF RANDOMLY ROUGH SURFACES

PACS: 43.28 En

Boulanger Patrice; Attenborough Keith
The University of Hull, Department of Engineering,
Hull HU6 7RX
Tel: 01482 466 600
E-mail: K.Attenborough@hull.ac.uk

ABSTRACT

The effects of the diffraction of sound waves by a randomly rough hard surface are modelled by an effective impedance. Measurements over surfaces containing randomly-spaced semi-cylinders and BEM predictions of Excess Attenuation spectra for random distributions are fitted for effective impedance roots by means of the classical theory for a point source above an impedance plane. Relations between effective impedance and frequency are deduced by usingTwersky's theory for small random semi-cylinders and by polynomial fitting.

INTRODUCTION

The objective of this work is to develop models of impedance as a function of frequency for various rough-hard surfaces corresponding to different sea states as part of research on sonic boom propagation. The main effect of surface impedance on sonic boom propagation is in the shadow zone. Less important effects are also in the primary carpet, where the incidence angle varies quite significantly. This work is focused on the grazing angle of the series of creeping waves diffracting into the shadow zone. The specific impedance of sea water is greater than that of air by four orders of magnitude, therefore the sea surface is considered to be acoustically hard for atmospheric sound propagation. The roughness will be considered static and the effect of the diffraction of sound waves by roughness is modelled as an effective admittance although, in reality, the scattered field is not constant because the boundary is continously in movement due to winds and currents.

THE ACOUSTIC MODELS

The Boundary Element Model (BEM)

The method used in this work was developed by Chandler-Wilde[1,2] who solved the Helmholtz equation for the pressure at the receiver with the boundary integral equation:

$$P(\vec{r},\vec{r}_0) = G_{\beta}(\vec{r}_0,\vec{r}) + \int_g \left\{ \frac{\partial G_{\beta}(\vec{r}_s,\vec{r})}{\partial n(\vec{r}_s)} - ik\beta(\vec{r}_s) G_{\beta}(\vec{r}_s,\vec{r}) \right\} P(\vec{r}_s,\vec{r}_0) ds(\vec{r}_s) \qquad (1)$$

where $P(\vec{r},\vec{r}_0)$ is the pressure at the point $\vec{r}$ when the source is at $\vec{r}_0$. The integral extends over the ground surface γ which is either the part of the surface impedance β lying above the horizontal or the part of the boundary with a normalized surface admittance $\beta(\vec{r}_s)$. $G_{\beta}(\vec{r}_0,\vec{r})$ is the Green function for the Helmholtz equation in a half plane with impedance boundary condition and can be calculated analytically. The boundary integral equation is solved approximately by discretizing the surface and assuming a constant pressure value in each boundary element of the ground surface. A flat or profiled ground surface can be modelled as the discretization points can be chosen out of the horizontal plane. Source, receiver and specular-reflection points are assumed to be in a vertical plane perpendicular to the roughness axis, and a line integral is solved. The BEM is used to predict sound levels over rough surfaces by including the roughness profile in the form of node coordinates input to the program. In all cases modelled in this work, the hard surfaces are assumed to have an admittance β=0. The BEM has proved to be an accurate model when compared to results from past

experiments involving mixed impedance[3] and rough ground[4]. The BEM is considered in this work as the reference to which the Twersky theory is compared.

Twersky's Theory

Twersky has developed a boss model[5,6,7,8] to describe coherent reflection from a hard surface containing semi-cylindrical roughnesses in which the contributions of the scatterers are summed to obtained the total scattered field. Sparse and closely-packed distributions of bosses have been considered and interaction between neighbouring scatterers has been included. His results lead to a real and imaginary part of the effective admittance of the rough hard surface which may be attributed respectively to incoherent and coherent scattering. The rough surface admittance depends on the incident wave number, the angle of incidence, the raised cross sectional roughness area per unit length, the dipole coupling between neighbour semi-cylindrical scatterer, and a packing factor introduced for random distributions. The authors have reported some success in the use of this model in the case of hard and soft roughness profiles [4,9]. Twersky's effective admittance model is subject to the approximation $ka<1$, where a is the radius of a cylindrical roughness. In this work, the number of roughness per unit length n, the semi-width of the semi-elliptical roughness e, the height of the roughness h_e, the minimum center-to-center separation distance between two roughness *minb* and the source height h_s are varied to obtain the best least square fit with the effective impedance obtained from BEM predictions or from measured data.

EXCESS ATTENUATION AND EFFECTIVE IMPEDANCE

Computation Method for Excess Attenuation

Excess attenuation is the attenuation of the sound wave in excess of that from spherical spreading and is computed from:

$$EA = 20\log\left|\frac{P}{P_1}\right| \tag{2}$$

where the direct wave is

$$P_1 = P_0\,\frac{\exp(ikR_1)}{R_1} \tag{3}$$

and where

$$P = P_0\,\frac{\exp(ikR_1)}{R_1} + QP_0\,\frac{\exp(ikR_2)}{R_2}. \tag{4}$$

The total pressure P for the BEM and the model based on Twersky's theory are computed from equations (1) and (4) respectively where R_1 and R_2 are the direct and reflected path distances. The model based on Twersky's theory incorporates the Weyl van der Pol spherical wave reflection coefficient Q.

Effective Impedance from Measured or Predicted Excess Attenuation

The Admittance Root Equation

The excess attenuation (EA) computed with the BEM from equations (1), (2) and (3) or observed in measurements corresponds to the attenuation due to the interference between the direct wave, the rough surface reflected wave and a possible surface wave. To estimate the effective impedance of such a rough surface it is considered that the complex EA measured or predicted by the BEM is produced by a flat surface of effective admittance β_{ef}. This impedance is found by solving for the admittance in the Weyl van der Pol spherical wave reflection coefficient. The problem becomes a β_{ef} – root search using the following equation at each frequency of interest

$$1+\frac{R_1}{R_2}e^{ik(R_2-R_1)}\left\{\frac{\cos\theta-\beta}{\cos\theta+\beta}+\left(1-\frac{\cos\theta-\beta}{\cos\theta+\beta}\right)\left(1+i\sqrt{\pi}\sqrt{ikR_2/2}\,(\beta+\cos\theta)e^{-\left(\sqrt{ikR_2/2}(\beta+\cos\theta)\right)^2}erfc(-iw(\beta))\right)\right\}-\frac{P}{P_1}=0 \tag{5}$$

where $F(w)$ is the sphericity factor. This equation does not have a readily available analytical solution, therefore, numerical methods have to be sought. Various numerical methods for finding the roots of complex variable equations have been implemented. The Newton Raphson method produces only one root per frequency point and has been used[10] previously in effective impedance

estimations. The second method uses an IMSL library routine based on Müller's technique and is limited practically to two roots for each frequency point. The weaknesses of these two methods are their potential lack of convergence toward a root for some frequency points, and the fact that they might miss important roots. The lack of convergence was an obstacle during several test cases, but an important factor in this work was the need to insure that no physically meaningful root was missed in the search. Therefore, a third more thorough root search method based on winding number integral has been developed.

The Winding Number Integral Method

This method is based on the winding number integral described by Brazier–Smith et al.[11] who apply it to the determination of roots from dispersion equations. If one seeks the roots of a function F, analytic everywhere inside a closed contour Γ, the difference between the number of zeros n_Z and the number of poles n_P of F inside Γ can be computed from the winding integral

$$\frac{1}{2\pi i}\oint_{\Gamma}\frac{F'}{F}dz = n_z - n_p \tag{6}$$

where the complex integral can be evaluated by the winding number of F(Γ) around the origin in an anticlockwise path. The winding number is noted by $n_Z - n_P$ = Wnd(F(Γ),0). Once the image of the closed contour Γ is computed by the function F the path can be divided into a series of chords and each cord is tested to check if it takes Ln(F) across the negative real axis. If it crosses from above, the winding number is increased by one and if from below, reduced by one. When the number of zeros inside a contour is established, the roots need to be identified. This work implements a search for two roots at a time in a contour, therefore only the first two moments of the winding integral are required. The expression of a moment I_n of order n is given by:

$$I_n = -\frac{1}{2\pi i}\left\{\left[z^n \ln F\right] - n\oint_{\Gamma} z^{n-1}\ln F dz\right\} = \sum_i \left(z_z^i\right)^n - \sum_j \left(z_p^j\right)^n \tag{7}$$

where z_z^i is the location of the ith zero and where z_p^j is the location of the jth pole. When the winding number is equal to one, the single zero is given by I_1 and when the winding number is equal to 2. The two zeros are determined by the roots of the quadratic equation

$$z^2 - I_1 z + 0.5(I_1^2 - I_2) = 0 \tag{8}$$

The integral shown in equation (7) is computed numerically with a Riemann sum. Great care has to be exercised when computing the function Ln(*F*) because Ln is not analytical across the negative real axis and the argument *F* of Ln might cross this branch cut. This potential discontinuity problem with Ln(*F(z)*) is solved using an analytical continuation of Ln across the branch cut. Mathematically, this means that instead of considering Ln as a simple function, it is viewed as a family of Ln functions each defined on a separate Riemanian sheet. This allows the continuity of the Ln(*F(z)*) family function at each branch cut, a branch cut being viewed as a seem of two successive Riemannian sheets. Therefore, when Arg(*F(z)*)=θ increases n times beyond π, Arg(*F(z)*)=θ + 2nπ, and one uses Ln(*F(Z)*) = Ln|*F(z)*| + iArg{*F(z)*} + 2nπi. When applied to the admittance root equation (5), the method uses a series of square contours Γ in which the roots are searched. If more than 2 roots are detected with the winding number count inside each square contour Γ, a smaller contour is chosen.

EXCESS ATTENUATION AND EFFECTIVE IMPEDANCE RESULTS FOR RANDOM DISTRIBUTIONS OF SEMI-CYLINDERS

In the following, d is the source-receiver separation distance, h is the source and receiver heights, h_{eff} is the effective source and receiver height, l is the semi-cylinder diameter and Z is the impedance.

Excess Attenuation Results for Small Hard Randomly Spaced Semi-Cylinders

The experimental procedure has been described in detail in other work[4] and only results are reported here. The measurements and BEM predictions used a 20 hard semi-cylinder roughness profile with l=0.0135m, d=1m and h=0.1m. Since the measured data and BEM predictions of excess attenuation spectra are rather sensitive to the roughness condition at the point of specular reflection between source and receiver, data and predictions are averaged over several random distributions. The averaged BEM prediction (Fig. 1.b) compares favourably with averaged

measured data (Fig. 1.a) for the excess attenuation spectra. It should be noted that the measured data are unreliable below 300 Hz.

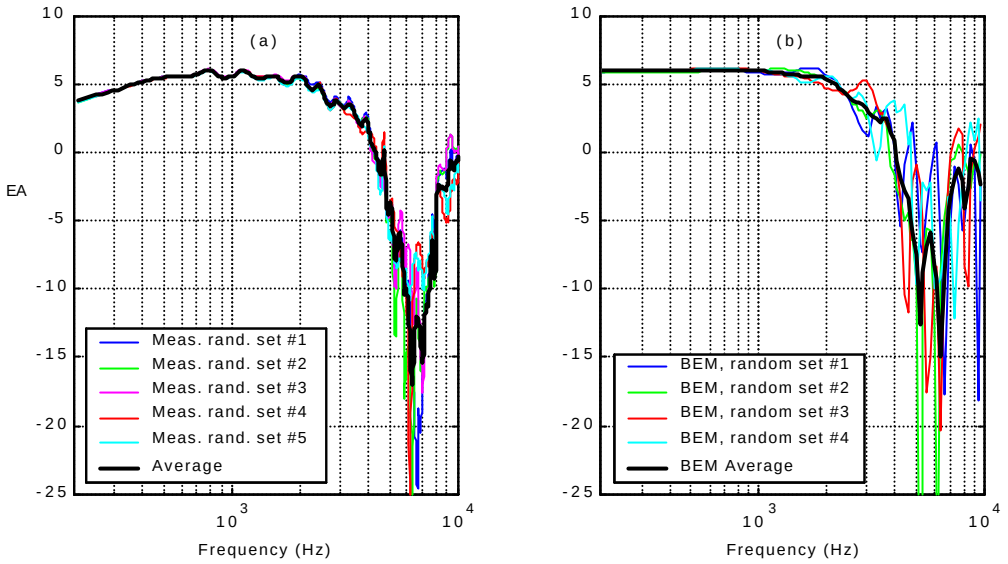

Fig. 1.- Measured (a) and BEM-predicted (b) excess attenuation spectra above a small semi-cylindrical roughness profile

Effective Impedance for Small Hard Randomly Spaced Semi-Cylinders

The winding number integral method results in only unphysical negative real impedance roots to equation (5) for some frequency points when using the nominal ground plane height with BEM predictions. The results are improved when the effective impedance is computed with a ground plane effective height set to the top of the random roughness (h_{ef}=0.093m). This step has been suggested before[12,13] and is applied in all effective impedance calculations from BEM predictions. Subsequently, any negative Re(Z) is set to zero. The latter step produces very little discrepancy between the nominal and deduced EA. The effective impedances deduced from measured data and BEM predictions are shown in Figure 2.a and 2.b. respectively. The predictions resulting from a 5-parameter least-square fit of Twersky's theory are shown as the thick-dashed and thick-solid line. A polynomial fit $\acute{a}f^{-1}$ is shown also as the thin-dashed and thin-solid line.

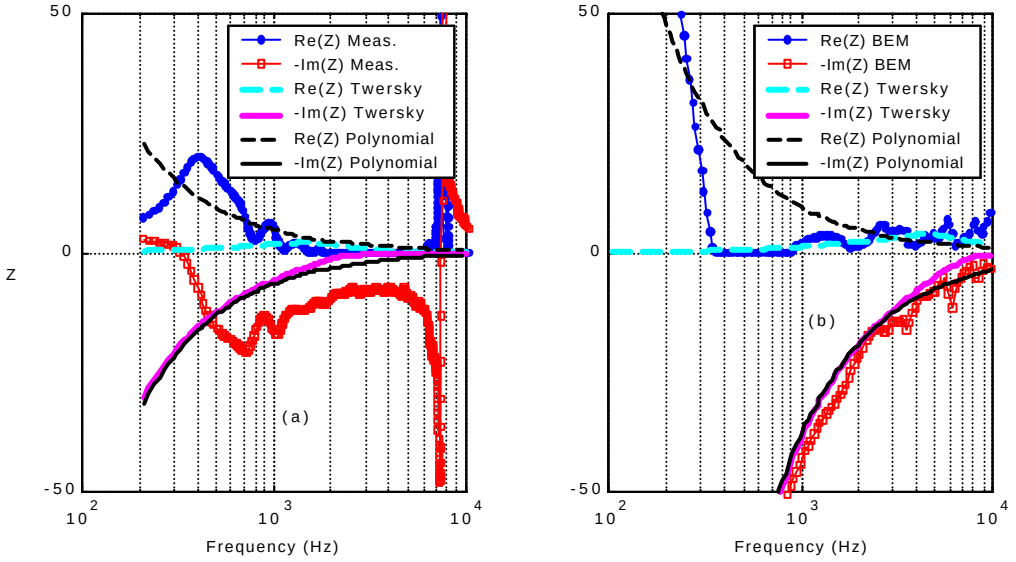

Fig. 2.- Effective impedance from measured (a) and BEM-predicted (b) excess attenuation above a small semi-cylindrical roughness profile

Excess Attenuation Results for Larger Randomly Spaced Semi-Cylinders

The measurements and BEM predictions are for a surface with a twelve hard semi-cylinder roughness profile with l=0.04m, d=1m and h=0.1m. The following graphs compare very favorably the BEM EA with measured data

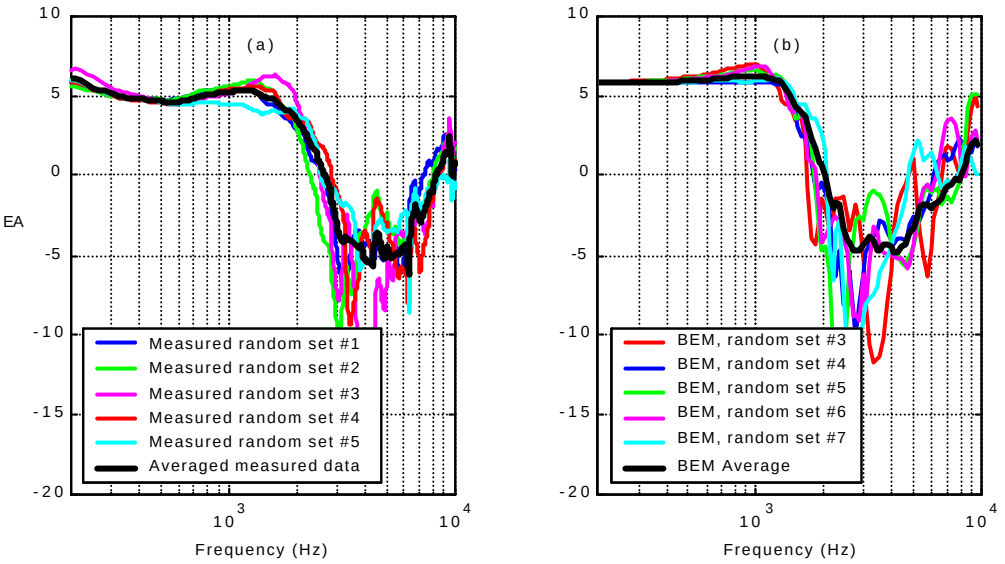

Fig. 3.- Measured (a) and BEM-predicted (b) excess attenuation spectra above a large semi-cylindrical roughness profile

Effective Impedance for Larger Randomly Spaced Semi-Cylinders

The effective impedance computed from the measured and BEM Excess Attenuation data are shown in figures 4.a and 4.b respectively. The results of a 5-parameter least-square fit using Twersky's theory is shown as the thick-dashed and thick-solid line. A similar polynomial fit $\acute{a}f^{-1}$ is shown also as the thin-dashed and thin-solid line.

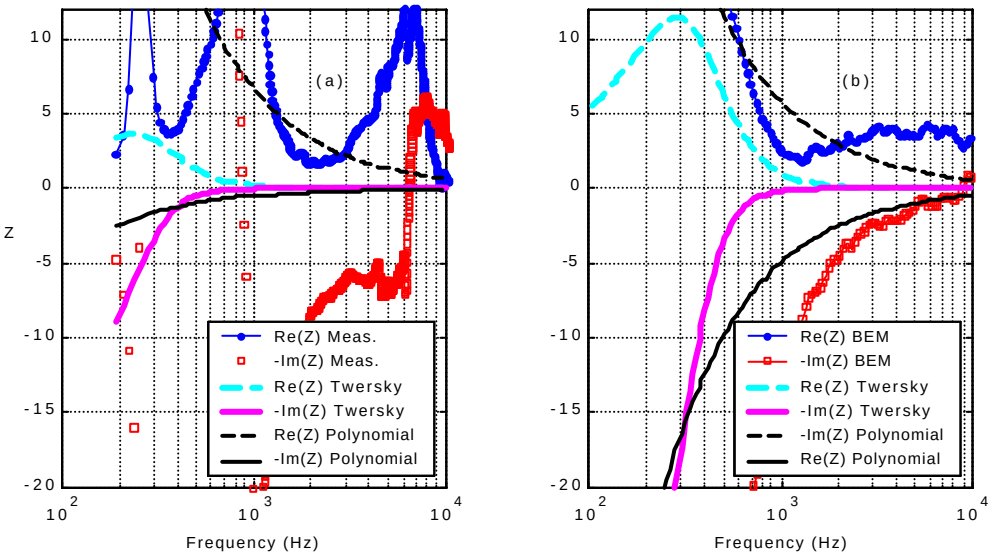

Fig. 4.- Effective impedance from measured (a) and BEM-predicted (b) excess attenuation above a large semi-cylindrical roughness profile

The values of the Twersky least square fit parameters found for the two roughness sizes and from the BEM prediction and measured data are summarized in Table 1.

	n (1/m)	e (m)	h_e (m)	$minb$ (m)	h_s (m)
BEM small cyl.	5	0.071	0.005	0.202	0.1
BEM large cyl.	1	0.071	0.1	0.142	0.1
Meas. small cyl.	3	0.137	0.005	0.336	0.1
Meas. large cyl.	1	0.137	0.1	0.274	0.1

Table 1 – Twersky's effective impedance least square fit parameters

The values of the polynomial fit coefficient for all cases studied are summarized in Table 2. As example of the notation, the column $Re(Z_m)_s$ shows results for the real effective impedance obtained from measurements in the case of small cylinders.

	$Re(Z_m)_s$	$Im(Z_m)_s$	$Re(Z_m)_l$	$Im(Z_m)_l$	$Re(Z_B)_s$	$Im(Z_B)_s$	$Re(Z_B)_l$	$Im(Z_B)_l$
á	4639	6574	6672	479	9471	38276	5840	4964

Table 2 – Coefficient of the effective impedance polynomial fit

CONCLUSIONS

The effective impedances of randomly rough surfaces have been deduced from complex excess attenuation obtained from either BEM predictions or measurements by finding the impedance roots of the Weyl van der Pol expression. These effective impedances can be used in a Weyl van der Pol expression that models a flat ground to reproduce the measured or BEM predicted excess attenuation. Satisfactory agreement is found between measured data and BEM predictions of Excess Attenuation using averaged data sets. It is found for BEM simulations that the effective impedance plane has to be raised to obtain physically meaningfull values of effective impedance real part. An analytical technique based on a boss theory from Twersky, where the contributions from randomly spaced semi-cylindrical or elliptical rough scatterers are summed to obtained the total scattered field, has been used also to fit the effective impedance from measurements and BEM predictions. The agreement between effective impedance from averaged measurements, from averaged BEM predictions and from Twersky's fit is better for the smaller cylinders. This is consistent with the small ka approximation implicit in Twersky's theory.

BIBLIOGRAPHICAL REFERENCES

[1] Chandler-Wilde S. N. and Hothersall D. C. "Efficient calculation of the green function for acoustic propagation above a homogeneous impedance plane ", J. Sound and Vib., **180**, 705-724 (1995).

[2] Chandler-Wilde S. N. and Hothersall D. C., "A uniformly valid far field asymptotic expansion of the green function for two-dimensional propagation above a homogeneous impedance plane" ", J. Sound and Vib., **182**, 665-675 (1995)

[3] Boulanger P., Attenborough K., Waters-Fuller T., and Li K. M. "Models and Measurements of Sound Propagation from a Point Source over Mixed Impedance Ground". J. Acoust. Soc. Am. **102**, 1432-1442 (1997).

[4] Boulanger P, Attenborough K., Taherzadeh S., Waters-Fuller T., and Li K. M., "Ground Effect Over Hard Rough Surfaces". J. Acoust. Soc. Am. **104**, 1474-1482 (1998).

[5] V. Twersky, "Scattering and reflection by elliptically striated surfaces" J. Acoust. Soc. Am. **40**, 883-895 (1966).

[6] V. Twersky, "Multiple scattering of sound by correlated monolayers" J. Acoust. Soc. Am. **73**, 68-84 (1983).

[7] V. Twersky, "Reflection and scattering of sound by correlated rough surfaces" J. Acoust. Soc. Am. **73**, 85-94 (1983).

[8] R. J. Lucas and V. Twersky, "Coherent response to a point source irradiating a rough plane" J. Acoust. Soc. Am. **76**, 1847-1863 (1984).

[9] Attenborough K. and Waters-Fuller T. , "Effective impedance of rough porous surfaces" J. Acoust. Soc. Am. **108**, 949-956 (2000).

[10] Taherzadeh S. and Attenborough K., "Deduction of ground impedance from measurements of excess attenuation spectra" " J. Acoust. Soc. Am. **105**, 2039-2042 (1999).

[11] Brazier –Smith P. R. and Scott J. F. M., "On the determination of the roots of dispersion equations by use of winding number integrals", J. Sound Vib. **145**, 503-510 (1991).

[12] Chambers J. P., Sabatier J. M. and Raspet R., "Grazing Incidence propagation over a soft rough surface", J. Acoust. Soc. Am. **102**, 55-59 (1997).

[13] Allard J.F., Kelders L. and Lauriks W., "Ultrasonic surface waves above a doubly periodic grating", J. Acoust. Soc. Am. **105**, 2528-2531 (1999).